Deciphering Systemic Wound Responses of the Pumpkin Extrafascicular Phloem by Metabolomics and Stable Isotope-Coded Protein Labeling[1][C][W]

Frank Gaupels*, Hakan Sarioglu, Manfred Beckmann, Bettina Hause, Manuel Spannagl, John Draper, Christian Lindermayr, and Jörg Durner

Institute of Biochemical Plant Pathology (F.G., C.L., J.Du.), Department of Protein Science (H.S.), and Institute of Bioinformatics and Systems Biology (M.S.), Helmholtz Zentrum München, German Research Center for Environmental Health, D–85764 Neuherberg, Germany; Institute of Biological Environmental and Rural Sciences, Aberystwyth University, Aberystwyth SY23 3DA, United Kingdom (M.B., J.Dr.); and Department of Cell and Metabolic Biology, Leibniz Institute of Plant Biochemistry, D–06120 Halle/Saale, Germany (B.H.)

In cucurbits, phloem latex exudes from cut sieve tubes of the extrafascicular phloem (EFP), serving in defense against herbivores. We analyzed inducible defense mechanisms in the EFP of pumpkin (*Cucurbita maxima*) after leaf damage. As an early systemic response, wounding elicited transient accumulation of jasmonates and a decrease in exudation probably due to partial sieve tube occlusion by callose. The energy status of the EFP was enhanced as indicated by increased levels of ATP, phosphate, and intermediates of the citric acid cycle. Gas chromatography coupled to mass spectrometry also revealed that sucrose transport, gluconeogenesis/glycolysis, and amino acid metabolism were up-regulated after wounding. Combining ProteoMiner technology for the enrichment of low-abundance proteins with stable isotope-coded protein labeling, we identified 51 wound-regulated phloem proteins. Two Sucrose-Nonfermenting1-related protein kinases and a 32-kD 14-3-3 protein are candidate central regulators of stress metabolism in the EFP. Other proteins, such as the Silverleaf Whitefly-Induced Protein1, Mitogen Activated Protein Kinase6, and Heat Shock Protein81, have known defensive functions. Isotope-coded protein labeling and western-blot analyses indicated that Cyclophilin18 is a reliable marker for stress responses of the EFP. As a hint toward the induction of redox signaling, we have observed delayed oxidation-triggered polymerization of the major Phloem Protein1 (PP1) and PP2, which correlated with a decline in carbonylation of PP2. In sum, wounding triggered transient sieve tube occlusion, enhanced energy metabolism, and accumulation of defense-related proteins in the pumpkin EFP. The systemic wound response was mediated by jasmonate and redox signaling.

A series of elegant experiments have demonstrated recently that phloem samples collected from cut petioles and stems of cucurbits do not represent pure fascicular phloem sap but rather the mixed content of extrafascicular phloem (EFP), xylem, and fascicular phloem (Zhang et al., 2010, 2012). The EFP is a unique feature of Cucurbitaceae. It consists of a complex network of longitudinal perifascicular strands next to the fascicular bundles, lateral commissural strands, and entocyclic as well as ectocyclic sieve tubes (Zhang et al., 2012). In contrast to the fascicular phloem, the EFP does not build effective callose plugs and freely exudes from cut sieve tubes. Due to easy sampling and its high protein content, cucurbit exudates were frequently used for phloem biochemistry (van Bel and Gaupels, 2004; Turgeon and Oparka, 2010; Atkins et al., 2011). Recently, more than 1,100 phloem proteins were identified in a large-scale proteomic approach with pumpkin (*Cucurbita maxima*; Lin et al., 2009). Interestingly, 67%, 46%, and 62% of the previously identified phloem proteins from rice (*Oryza sativa*), rape (*Brassica napus*), and castor bean (*Ricinus communis*), respectively, were found among the EFP proteins of pumpkin, confirming functional overlap between extrafascicular and fascicular phloem of different plant species (Lin et al., 2009).

Although the EFP is physically and functionally linked to the fascicular phloem, a role in assimilate transport, the major function of fascicular phloem, is still ambiguous. The presence of many defense-related proteins in cucurbit phloem exudates rather pointed toward a role of the EFP in (systemic) stress and defense responses (van Bel and Gaupels, 2004; Walz et al., 2004; Turgeon and Oparka, 2010). In this regard, it has been largely overlooked by phloem biologists that phloem exudates of cucurbits are routinely classified by ecologists as latex-like exudates involved in

[1] This work was supported by the Deutsche Forschungsgemeinschaft (grant no. GA 1358/3–1 to F.G.).

* Corresponding author; e-mail frank.gaupels@helmholtz-muenchen.de.

The author responsible for distribution of materials integral to the findings presented in this article in accordance with the policy described in the Instructions for Authors (www.plantphysiol.org) is: Frank Gaupels (frank.gaupels@helmholtz-muenchen.de).

[C] Some figures in this article are displayed in color online but in black and white in the print edition.

[W] The online version of this article contains Web-only data.

www.plantphysiol.org/cgi/doi/10.1104/pp.112.205336

defense against herbivorous insects (Carroll and Hoffman, 1980; Tallamy, 1985; Konno, 2011). In fact, the EFP is similar to branched laticifer (latex-containing conduits) networks, which develop from protophloem and/or phloem initials (Hagel et al., 2008). For this reason, and for better differentiation from fascicular phloem samples, hereafter we will use the term phloem latex instead of phloem exudates.

Phloem latex provides two layers of defense. It is a physical barrier for small insects, which can be trapped in large droplets of exudates from wounded veins or sticky compounds that might glue their mouth parts (Konno, 2011). In addition, it was also shown that compounds in phloem latex of squash (*Cucurbita* spp.) such as cucurbitacin steroids deterred beetles from feeding (Carroll and Hoffman, 1980; Tallamy, 1985). Specialist feeders of cucurbits can tolerate toxic compounds in phloem latex or even use them for their own defense. Other herbivores, such as certain species from the genus *Epilachna*, counteract chemical defense by trenching. They isolate a circular leaf area by cutting all tissues except for the lower epidermis, this way avoiding pressure-driven exudation within the feeding area (Carroll and Hoffman, 1980; Tallamy, 1985; Konno, 2011).

Some defense responses were demonstrated to be inducible by herbivore attack both in the local as well as neighbor leaves (Carroll and Hoffman, 1980; Tallamy, 1985). In this report, we analyzed by gas chromatography/mass spectrometry (GC-MS) and stable isotope-coded protein labeling (ICPL) systemic wound responses of the EFP upon leaf wounding. Overall, wounding induced jasmonate accumulation, reprogramming of the metabolism toward increased energy status, and the regulation of proteins related to carbon metabolism, signaling, and defense. This report gives a comprehensive overview of wound-inducible changes in the metabolite and the protein composition of pumpkin phloem latex, thereby providing a framework for future in-depth studies on defense responses of both EFP as well as fascicular phloem.

RESULTS

For a long time, phloem latex has been used in biochemical studies assuming that it is equivalent to fascicular phloem sap. However, separate sampling of EFP and fascicular phloem exudates of pumpkin using microdissection revealed large differences in the sugar and protein composition between both phloem systems (Zhang et al., 2010). In this report, this finding was confirmed by employing aphid stylectomy for the collection of pure phloem sap (Gaupels et al., 2008a, 2008c). Pumpkin stylet exudates were compared with exudates from cut petioles and stems displaying different SDS-PAGE band patterns between the two sample types (Fig. 1). Particularly, the major phloem proteins (PP1 and PP2), which account for more than 80% of the total protein content in phloem latex, are virtually absent in stylectomy exudates, whereas prominent proteins of about 32 and 60 kD in stylectomy samples

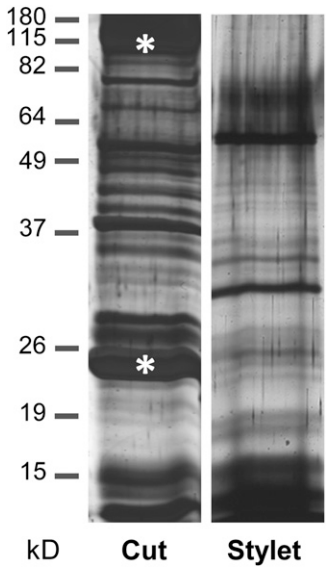

Figure 1. Protein patterns are different between phloem latex collected from cut petioles and stems as compared with phloem sap collected from cut aphid stylets. Each 1.5-μL phloem sample was analyzed by SDS-PAGE and silver staining. Asterisks indicate the major phloem proteins PP1 (96 kD) and PP2 (24 kD).

are not abundant in phloem latex. Together, these and previous results suggest that phloem latex is indeed not equivalent to fascicular phloem sap.

As discussed below, proteins and metabolites in pumpkin phloem latex collected within the first few minutes after cutting the petiole or stem originate predominantly from the EFP. Therefore, we wounded the leaves of pumpkin plants and sampled phloem latex within 2 min after cutting in order to analyze wound-inducible defense mechanisms of the EFP.

Leaf Wounding Induces the Accumulation of Jasmonates in the EFP

Wounding was performed by crushing the edges of all leaves for induction of a uniform and reproducible systemic response in the EFP of petioles and stems (Fig. 2A). The well-known wound signals jasmonic acid (JA) and its conjugate JA-Ile were not found in phloem latex from control plants but were detected at 30 min and peaked at 60 min after wounding, reaching maximum concentrations of 107 nM JA and 49 nM JA-Ile (Fig. 2B). The jasmonate levels strongly decreased again at 3 h after treatment. We also found jasmonate and/or wound-responsive proteins in phloem latex, which is discussed below. These results argue for the onset of a systemic wound response in the EFP.

Transient Reduction of Phloem Exudation Correlates with the Formation of Saccharide Polymers

Leaf damage induced a transient decrease in exudation volume by about 30% at 0.5-, 1-, and 3-h time points (Fig. 3A). The reduced exudation correlated with

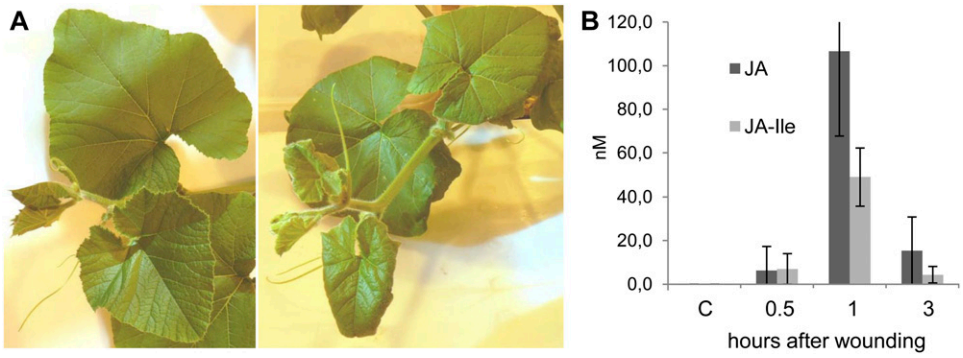

Figure 2. Leaf wounding induced the accumulation of jasmonates in pumpkin phloem latex. A, All leaves of a plant were wounded at the edges for induction of a uniform response throughout the aerial plant parts. A control plant (left) and a wounded plant at 3 h after wounding (right) are shown. B, JA and JA-Ile were not detected in phloem latex from untreated pumpkin plants but accumulated at 0.5, 1, and 3 h after wounding of all leaves. Error bars indicate the SD of three independent replicates. Every replicate was a pool of phloem exudates from seven to 10 plants. C, Control. [See online article for color version of this figure.]

an accumulation of "sticky compounds" in phloem latex, which caused the plugging of pipet tips during the sampling procedure. At 48 h after wounding, the exudate volume increased above control levels and phloem latex was even less sticky than control samples. Results of HPLC fractionation combined with flow injection electrospray ionization (FIE)-MS analysis suggested that the sticky compounds are saccharide polymers (Fig. 3B). The exact nature of the saccharide polymers is not resolved, but they consist of sugar units of 162 mass-to-charge ratio (dehydrated Glc) bound to an unknown conjugate. Most likely, wounding induced the synthesis of glucans such as callose.

Energy Status, Suc Transport, Carbohydrate Metabolism, and Amino Acid Synthesis Are Enhanced after Wounding

The ATP level is a widely used measure for cellular energy status (Geigenberger, 2003). Leaf wounding of pumpkin triggered only a slight, nonsignificant depression at 0.5 and 1 h but a significant 17% rise in ATP concentrations from 6 to 24 h after treatment (Fig. 4).

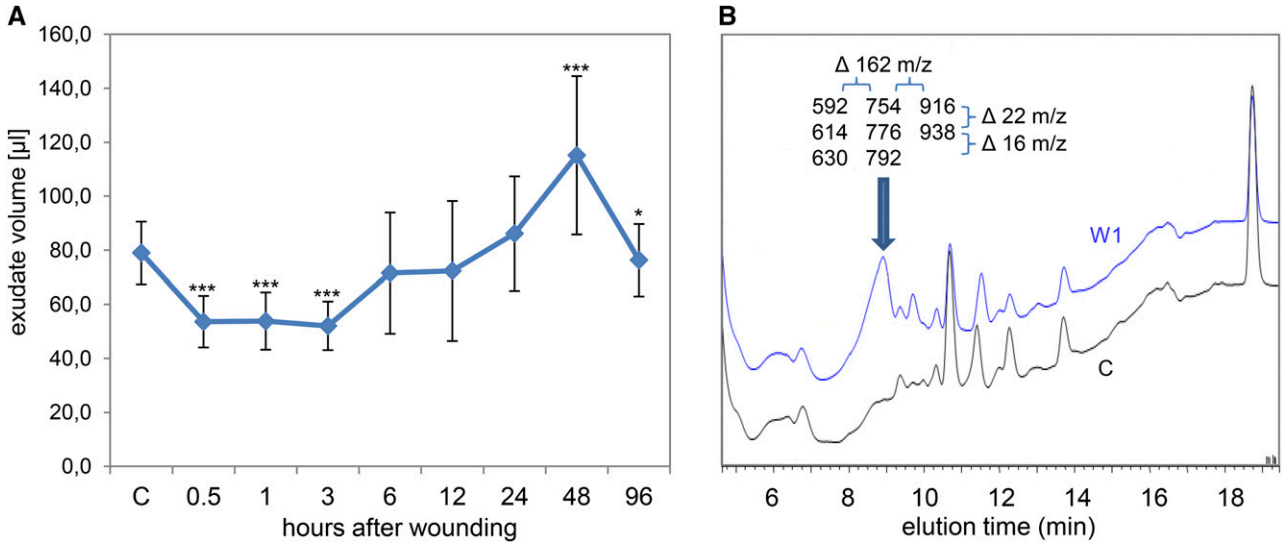

Figure 3. The volume of pumpkin phloem exudates changes concurrent with an accumulation of polysaccharides upon leaf wounding. A, The exudate volume decreased transiently at 0.5, 1, and 3 h after wounding of all leaves. Error bars indicate the SD of 13 replicates. Asterisks indicate statistically significant differences from control samples from untreated plants (Student's *t* test, $*P < 0.05$; $***P < 0.001$). B, The decrease in volume correlated with an accumulation of polysaccharides in the exudates at 1 h after wounding (W1; top curve), probably representing callose formation. The HPLC fractions containing the peak marked by the arrow were analyzed by FIE-MS. Resulting masses (mass-to-charge ratio [*m/z*]) are shown. Note the mass differences of 162 (one sugar unit) between columns and 22 (protonated versus sodium adduct) or 16 (sodium versus potassium adduct) between rows of displayed masses. C, Control. [See online article for color version of this figure.]

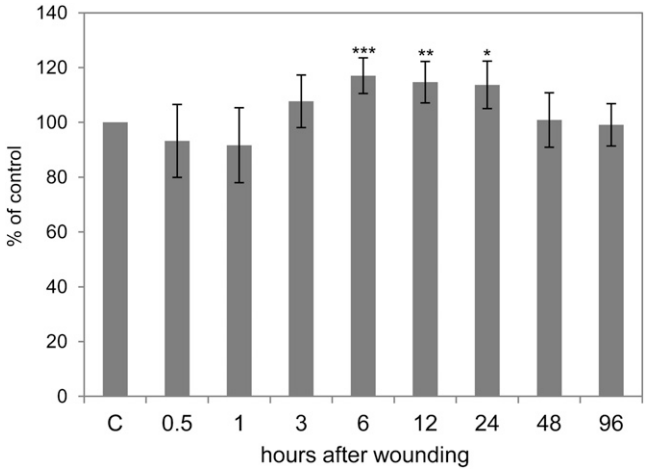

Figure 4. ATP levels as a measure of cellular energy status increase after wounding. Error bars indicate the SD of six replicates. Asterisks indicate statistically significant differences from control samples from untreated plants (Student's *t* test, $*P < 0.05$; $**P < 0.01$; $***P < 0.001$). C, Control.

Energy metabolism is fueled by Suc, which is the major transport sugar in most plants. ATP is then generated during glycolysis, the citrate cycle, and mitochondrial electron transport. GC-MS data imply that Suc accumulates in the EFP after wounding (Fig. 5). Also, intermediates of glycolysis (Glc-6-P) and the citrate cycle (pyruvate, citrate, and malate) increased. Phosphate, which is released during glycolysis and the citrate cycle, shows kinetics remarkably similar to citrate, malate, and Glc-6-P, with an early peak at 3 h after wounding, confirming the functional link between these metabolites. 3-hydroxypropionate levels are also strongly elevated after wounding, whereas the closely related lactate (2-hydroxypropionate) is not consistently regulated (Fig. 5; Supplemental Fig. S1). Myoinositol decreased after wounding. In sum, the elevated ATP levels in response to crushing of the leaf edges most likely arose from stimulated glycolysis, the citrate cycle, and mitochondrial electron transport.

Under stress conditions, energy/ATP is utilized for the production of defensive compounds such as callose, various stress signals, and defense-related proteins. Accordingly, after wounding, we observed a general increase in amino acids, which probably served as building blocks for enhanced protein and secondary metabolite synthesis (Supplemental Fig. S2).

Proteins Related to Signaling, Defense, Protein Metabolism, and Transport Processes Are Wound Regulated

In initial experiments, two-dimensional electrophoresis was applied for the identification of wound-regulated phloem latex proteins. However, results obtained with this method were unreliable, mainly due to uncontrolled precipitation of PP1/PP2 during isoelectric focusing, which caused heavy streaking, as also observed previously by others (Walz et al., 2004; Malter and Wolf, 2011). Specific problems related to electrophoresis can be avoided by gel-free techniques such as ICPL combined with MS. A principal problem with this approach was masking of less-abundant proteins by a few major proteins, resulting in poor labeling efficiency and a very restricted number of protein identifications. Recently, combinatorial hexapeptide ligand libraries bound to chromatographic beads (ProteoMiner) were used for the depletion of high-abundance proteins and the enrichment of low-abundance proteins in plant extracts (Fröhlich and Lindermayr, 2011; Fröhlich et al., 2012). Application of ProteoMiner to phloem latex caused a considerable change in protein pattern (Supplemental Fig. S3; Fröhlich et al., 2012). Major proteins such as PP1 and PP2 and total protein concentrations were strongly reduced, while new bands probably representing less abundant proteins appeared on the gel.

Combining ProteoMiner pretreatment with ICPL, we found that wounding induced a reprogramming of the phloem latex proteome, with altogether 51 proteins being modulated after leaf crushing (Table I; Supplemental Table S1). Six proteins were part of the carbohydrate and energy metabolism. For instance, GDP-L-Fuc synthase and UDP-L-Rha synthase, which both use nucleotide sugars for cell wall synthesis, were repressed after wounding. Also, Glc-6-P dehydrogenase, which synthesizes the first step of the pentose phosphate pathway, displayed a 3-fold decrease in abundance. The proteomic approach uncovered three proteins that might be key

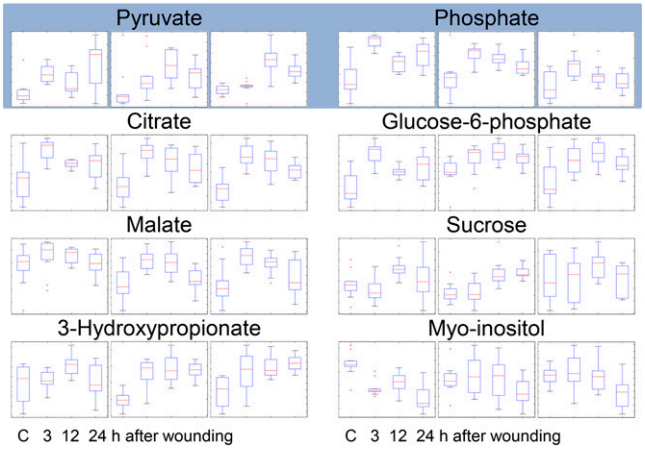

Figure 5. Energy and carbohydrate metabolism are enhanced after wounding. Phloem latex from untreated control and wounded plants at time points 3, 12, and 24 h after wounding were analyzed by GC-MS/MS. The results of three independent experiments with 11 biological replicates are shown. Box plots derived from ANOVA represent relative signal intensity ratios. Pyruvate and phosphate species (shaded) are central metabolites of the citric acid cycle (citrate and malate) and glycolysis/gluconeogenesis (Glc-6-P, Suc, and myoinositol). 3-hydroxypropionate is related to pyruvate (2-oxoproprionate) and lactate (2-hydroxypropionate) and is involved in energy metabolism, glycolysis, and Ala synthesis. C, Control. [See online article for color version of this figure.]

Table I. *Wound-regulated proteins in phloem latex identified by isotope-coded protein labeling*

MW, Molecular mass in kD.

Accession[a]	MW	W3/C[b]	W24/C[b]	Description
Carbohydrate and energy metabolism				
429162	31.1	2.21	2.49	14-3-3 protein 32-kD endonuclease
Cucsa.089980	35.9	0.72	0.58	GDP-L-Fuc synthase
Cucsa.302670	33.6	0.33	0.33	UDP-L-Rha synthase
Csa022482	59.2	0.33	0.43	Glc-6-P dehydrogenase
Cucsa.170120	40.9	0.59	0.62	SNF1-related protein kinase2
1743009	57.8	0.09	0.09	SNF1-related protein kinase1
Signaling, defense				
10998336	48.1	3.25	4.06	Silverleaf whitefly-induced protein1
113045960	17.9	1.09	1.69	MAPK6
319439585	33.8	0.79	1.70	Cyclin-dependent kinase A
110748608	42.7	1.07	1.63	NO_3^- stress-induced MAPK
117573664	16.5	1.82	4.13	16-kD phloem protein1, PP16-1
1753099	95.3	1.06	2.09	Phloem filament protein, PP1
508445	24.5	0.47	1.09	Dimeric phloem-specific lectin, PP2
99906997	35.6	0.59	1.15	Class III peroxidase precursor
20453013	64.0	0.61	0.90	Phloem calmodulin-like domain protein kinase
Cucsa.142500	16.9	0.83	0.56	Calmodulin
50262213	7.6	0.50	1.09	Putative chymotrypsin protease inhibitor
Chaperones				
Csa001697	79.9	2.24	2.67	HSP81
Cucsa.142610	60.5	1.78	2.27	Chaperonin-containing complex protein1
Csa009634	59.0	1.43	2.00	T-complex protein1 subunit ζ-like
62728587	18.1	1.08	1.73	Cyclophilin
Cucsa.106590	13.2	0.96	0.59	Peptidyl-prolyl cis-trans-isomerase Pin1
51477394	63.8	0.57	1.21	Protein disulfide isomerase (PDI)-like protein3
Protein synthesis and degradation				
Cucsa.153230	67.1	3.23	1.38	DEAD box RNA helicase
Cucsa.162420	53.5	1.42	1.72	DEAD box RNA helicase
Cucsa.345110	85.1	2.04	2.42	Elongation factor2-like
Cucsa.201940	16.6	2.40	1.66	Ubiquitin-conjugating enzyme E2
Cucsa.181800	48.0	2.11	2.64	26S protease subunit 6A-like
81076307	16.5	1.63	2.00	Putative translation initiation factor eIF-1A-like
224110244	17.5	0.98	1.81	Proteasome subunit α type 2
224085688	26.6	1.05	1.79	Proteasome subunit α type 1
Csa011709	86.7	1.58	1.77	Cullin-1
147800085	66.7	0.53	1.26	E3 ubiquitin ligase ARI7-like
224095561	97.6	0.58	1.13	26S proteasome regulatory complex component
Cucsa.018140	51.2	0.60	0.78	Eukaryotic translation initiation factor3 subunit 6N
Cucsa.342220	45.3	0.64	0.48	COP9 signalosome subunit4-like
307136429	25.5	0.41	0.34	COP9 signalosome subunit7a
298352997	17.2	0.31	0.36	Putative ubiquitin-conjugating enzyme
Transport, cytoskeleton				
495731	23.0	2.38	1.79	Small ras-related
6097869	13.8	0.93	3.52	Actin
Csa010390	41.7	1.71	1.26	Actin
Cucsa.053580	17.1	2.18	1.59	Actin-depolymerizing factor
157467219	18.5	2.44	1.73	GTP-binding nuclear protein Ran3-like
307135957	49.5	0.61	1.81	Tubulin α-chain
123192431	25.3	1.43	1.89	Ran1
137460	68.8	0.83	1.73	V-type proton ATPase catalytic subunit A
255570599	96.4	0.53	1.01	Importin β-1, putative
51477379	99.8	0.52	1.26	DRP, dynamin
Others				
Cucsa.328440	43.2	1.53	1.71	*S*-Adenosyl-Met synthetase
307135934	32.9	1.70	1.06	Pyridoxal biosynthesis protein
168049525	89.6	0.55	1.18	Cell division control protein48, CDC48

[a]Accession numbers from the National Center for Biotechnology Information, International Cucurbit Genomics Initiative (Csa identifiers), and the Joint Genome Institute (Cucsa identifiers). [b]C, W3, W24 indicate phloem latex from untreated control plants or wounded plants at 3- and 24-h time points.

regulators of energy and carbohydrate metabolism. Two Sucrose-Nonfermenting1 (SNF1)-related protein kinases, SnRK1 and SnRK2, were 11- and 1.67-fold repressed upon the stress treatment, while the 14-3-3 protein 32-kD endonuclease present in phloem latex was 2-fold induced by wounding.

Proteins with roles in signaling and defense included the Silverleaf Whitefly-Induced Protein1 (SLW1), which was 3- and 4-fold induced at 3 and 24 h after wounding, respectively. Also, three kinases related to stress signaling, namely the NO_3^- stress-induced mitogen-activated protein kinase (MAPK), cyclin-dependent kinase A, and MAPK6, were induced at the later time point. Among the major phloem proteins, PP2 was 2-fold down-regulated at 3 h, whereas the 16-kD Phloem Protein1 (PP16-1) and PP1 were up-regulated. Chaperones modify protein structure and function and are often involved in signaling processes. Heat Shock Protein81 (HSP81) belongs to the HSP90 family and is 2- and 3-fold induced at the two sampling time points. Moreover, an 18-kD cyclophilin (CYP18) was more abundant at 24 h after wounding as compared with the control. CYP18 turned out to be an excellent marker for stress responses of the EFP, as detailed below.

Fifteen wound-regulated proteins are related to protein synthesis and degradation (Table I), consistent with previous reports that pumpkin phloem latex contains the complete machinery for protein turnover (Lin et al., 2009; Fröhlich et al., 2012). In general, regulation of these proteins mainly reflects proteomic reprogramming under stress conditions. Enhanced metabolism and protein turnover correlated with an increase in transport processes, as indicated by the accumulation of transport-related proteins such as the small GTPases Ran1, Ran3, and small Ras-related, a vacuolar-type proton ATPase, and elements of the cytoskeleton, including two actin isoforms, an actin-depolymerizing factor, and tubulin. Dynamin, which is involved in the scission of vesicles from membranes, decreased after wounding.

Some proteome changes were readily visible after SDS-PAGE separation of phloem latex proteins (Fig. 6). PP2

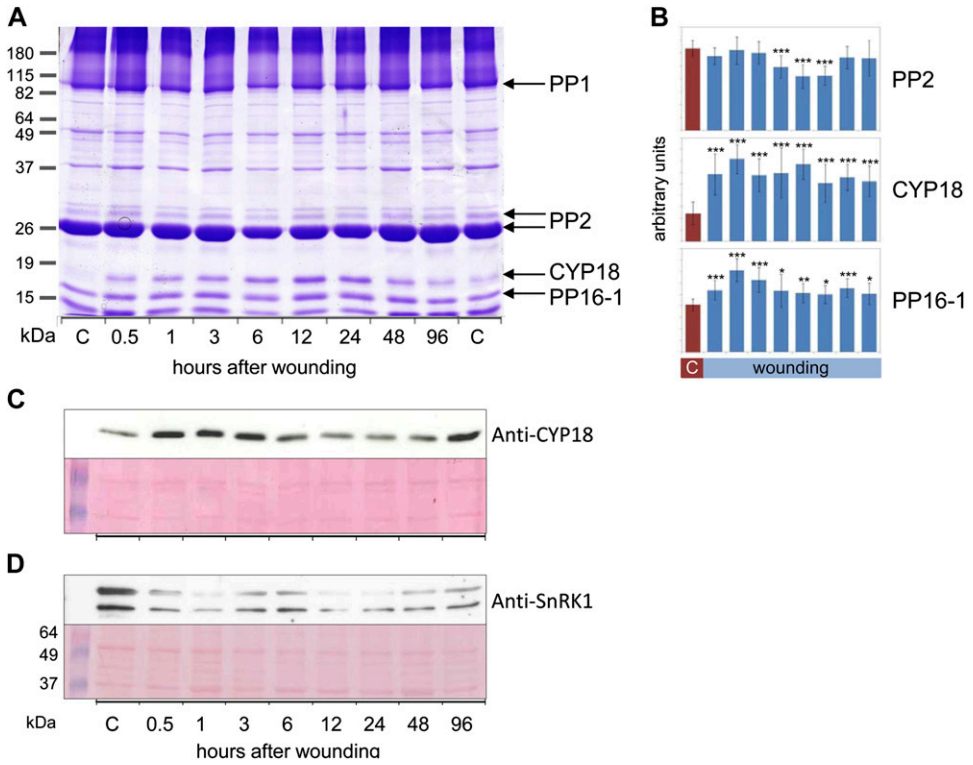

Figure 6. PP2, CYP18, PP16-1, and SnRK1 are wound-regulated phloem proteins. A, Representative Coomassie blue-stained polyacrylamide gel displaying phloem proteins from untreated (two controls shown) or wounded pumpkin plants. Major phloem proteins PP1 and PP2, PP16-1, and CYP18 were labeled. CYP18 and PP16-1 were cut from the gel and identified by LC-MS/MS. B, Quantification of PP2 (major isoform), CYP18, and PP16-1 band intensities by ImageJ. Note the transient reduction in PP2 band intensity at 6 to 24 h after wounding, whereas CYP18 and PP16-1 were significantly induced from 0.5 to 96 h after wounding. Error bars indicate SE ($n = 9$). Asterisks indicate statistically significant differences from the control (Student's t test, $^*P < 0.05$; $^{**}P < 0.01$; $^{***}P < 0.001$). C, Western-blot analysis of phloem proteins with anti-CYP18 antibodies confirmed the wound induction of CYP18, although the kinetics is induction are somewhat variable. D, Western-blot analysis of phloem proteins with anti-SnRK1 antibodies. The western-blot signal corresponds to the expected protein mass of approximately 57 kD. The identity of the bottom band is unknown. The nitrocellulose membrane was stained with Ponceau red for confirmation of equal loading. C, Control. [See online article for color version of this figure.]

levels decreased between 6 and 24 h after wounding (Fig. 6, A and B). Intraexperimental variability might explain why in the ICPL approach, PP2 decreased already at 3 h but not at 24 h. However, the general tendency of regulation was the same with both techniques. Another major phloem protein, PP16-1, was found by ICPL to be induced after wounding, and this was confirmed by quantification of SDS-PAGE results (Fig. 6B). The most prominent wound-responsive protein was unequivocally identified by SDS-PAGE, liquid chromatography-tandem mass spectrometry (LC-MS/MS), and western-blot analyses to be an 18-kD cyclophilin (Fig. 6, A–C). CYP18 abundance increased already at 0.5 h and was still higher than the control level at 96 h. This is in accordance with the results of the ICPL experiment, in which CYP18 was also up-regulated, although only at 24 h after wounding. Additionally, we confirmed the regulation of SnRK1, which was shown to be strongly down-regulated both by ICPL and western-blot analyses (Fig. 6D). In sum, we were able to validate the results of the ProteoMiner/ICPL experiment by SDS-PAGE and western-blot analyses with nonpretreated phloem latex. Although the extent and timing were somewhat variable, the general tendencies of the regulation of the tested candidate wound-responsive proteins were consistent between the different experimental approaches.

Wounding Triggers Redox Modifications of Phloem Proteins

If phloem latex is exposed to air oxygen, it will gelate within a few hours. This special feature of cucurbit phloem latex is mediated by the redox-sensitive PP1 and PP2, which polymerize upon oxidation of Cys residues (Read and Northcote, 1983). Gelation can be artificially induced by 4-fold dilution of phloem latex with alkaline buffer (Alosi et al., 1988). By using this assay, we found that sample gelation was significantly delayed at 6 to 48 h after leaf crushing (Fig. 7). The average gelation time rose from 5 min in control samples to 22 min at 12 h after treatment. In order to investigate if PP1 and PP2 were altered in their redox state, western-blot analysis for the detection of carbonylated proteins was performed (Fig. 8). PP1 was not carbonylated, whereas PP2, CYP18, and PP16-1 produced strong signals on the western blot. Surprisingly, the signals for two PP2 isoforms were already strong in control samples but weakened from 6 to 96 h after wounding, with minimum signal intensity at the 12-h time point. However, only weak changes in protein abundance of PP2 were observed by Ponceau staining, implying that the western-blot signals decreased due to decarbonylation of PP2 rather than reduction in PP2 protein levels. For CYP18 and PP16-1, we observed a good correlation between the intensities of western-blot signals and Ponceau staining, suggesting that the oxidation status of these proteins did not change after wounding.

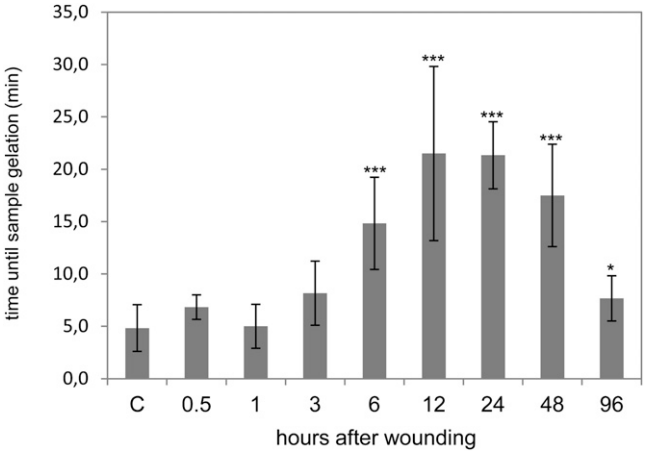

Figure 7. The gelation of phloem latex due to redox-dependent polymerization of PP1 and PP2 is delayed after wounding. The time until sample gelation was measured after the addition of 3 volumes of alkaline buffer (pH 7.8). In this assay, samples were assumed to be gelated when they could not be mixed by vortexing anymore. Error bars indicate SE ($n = 9$). Asterisks indicate statistically significant differences from the control (Student's t test, $^*P < 0.05$; $^{***}P < 0.001$). C, Control.

DISCUSSION

Pumpkin Phloem Latex Mainly Originates from the EFP

Phloem latex does not represent pure EFP exudates, since it is blended with fascicular phloem and xylem/apoplastic fluids (Zhang et al., 2012). The contribution of the vascular systems to the latex composition varies between cucurbit species. For example, a major proportion of initial phloem exudates from cucumber (*Cucumis sativus*) originated from the fascicular phloem (Zhang et al., 2012). On the other hand, pumpkin phloem exudates collected within the first minutes after cutting of stems and petioles mainly consisted of EFP content. This was suggested by several observations. (1) Microscopy revealed that phloem sap exuded freely from the EFP but only a little from the fascicular phloem, which was shown to be rapidly occluded by callose formation (Zhang et al., 2010, 2012). (2) Nonmobile hexoses, which are not present in pure fascicular phloem sap, were detected in phloem latex, whereas levels of the major phloem-mobile carbohydrates stacchyose and Suc were exceptionally low (Zhang et al., 2010, 2012). (3) Protein concentration and composition were disparate between fascicular phloem exudates and phloem latex (Fig. 1; Zhang et al., 2010). The above-mentioned facts would argue against an important contribution of fascicular phloem sap to pumpkin phloem latex.

Feeding experiments with xylem-mobile silicon showed that phloem latex was diluted by xylem fluid (Zhang et al., 2012). According to a current model, cutting releases the pressurized EFP content, and exudation of phloem latex is driven by diffusion of water into the EFP, causing an increase in turgor pressure (Zhang et al., 2012; Zimmermann et al., 2012). However,

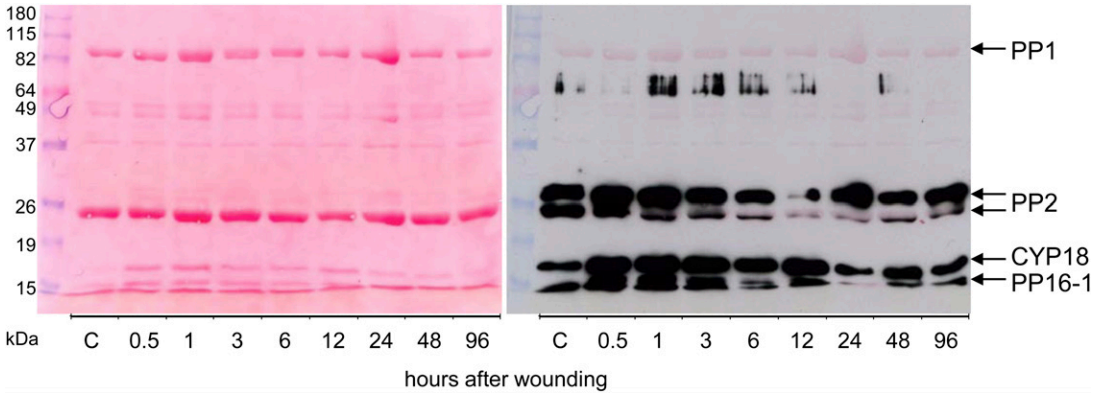

Figure 8. Leaf wounding triggers a specific decline in carbonylation of PP2. Carbonylated (oxidized) phloem proteins were labeled with DNP for immunodetection by anti-DNP antibodies. The left image shows Ponceau red-stained proteins after blotting to a nitrocellulose membrane. The right image is a digital overlay of the western-blot signals with Ponceau red-stained proteins. Note that CYP18, PP16-1, and PP2 isoforms but not PP1 cross reacted with anti-DNP antibodies. C, Control. [See online article for color version of this figure.]

translocation of water from the xylem (i.e. apoplast) through membranes or aquaporins into the EFP sieve tubes would probably not permit the exchange of large solutes between both vascular systems. Therefore, xylem proteins and metabolites are most likely only trace constituents of phloem latex. This is also inferred from the low protein concentrations of 0.05 to 0.1 μL mL^{-1} in xylem sap (Buhtz et al., 2004) as compared with more than 20 μL mL^{-1} in phloem latex. Efflux of phloem latex will cease after some minutes, and subsequently, xylem sap will exude if the root pressure is high enough (Zhang et al., 2012; Zimmermann et al., 2012). On these grounds, we sampled EFP-enriched phloem latex by immediate blotting of the cut surface with lint-free paper (to remove the content of damaged nonvascular cells and fascicular phloem sap) and collection of exudates within less than 2 min after cutting (to avoid further sample dilution by xylem exudation). In sum, phloem latex from pumpkin consists predominantly of diluted EFP content with trace materials from other sources and can be employed for analyzing the EFP wound response.

Is the Systemic Wound-Induced Accumulation of Saccharide Polymers in Phloem Latex Related to Sieve Tube Occlusion?

Sieve tubes of the fascicular phloem contain valuable nutrients. To avoid loss of phloem content from wounded veins, most plants have developed rapid and reversible sieve tube occlusion by callose formation. The EFP was presumed to be devoid of this defense mechanism, since it exudes large volumes of phloem latex from cuts (van Bel and Gaupels, 2004; Turgeon and Oparka, 2010; Atkins et al., 2011). However, during sampling, we observed a transient reduction by about 30% in phloem latex exudation at 0.5 to 3 h after wounding, concurrent with an accumulation of sticky compounds, which were identified as saccharide polymers. Similar compounds were previously detected in pumpkin phloem latex, without biological functions being investigated (Tolstikov and Fiehn, 2002). Taken together, these observations are reminiscent of callose formation in the fascicular phloem. It remains to be answered why, in the EFP wound-induced sieve tube, occlusion is obviously ineffective.

One possible explanation is that sieve tubes as well as sieve plates of the EFP are exceptionally wide and, therefore, are difficult to seal by callose (Mullendore et al., 2010; Zhang et al., 2012). More likely, however, exudation of copious amounts of phloem latex is a defensive trait (Turgeon and Oparka, 2010; Konno, 2011). In general, latex is particularly effective in defense against small insects, which are confronted at the site of feeding with relatively large droplets of the toxic and sticky liquid (Konno, 2011). Insects can counteract this defense by trenching and vein cutting. The resulting release of pressure from laticifers allows the insects to feed in the now unprotected parts of the leaf for a certain time interval. Only after occlusion and reestablishment of high-pressure conditions can damaged laticifers exude latex again (Konno, 2011).

EFP sieve tubes have typical features of laticifers in that they are under high pressure and exude large volumes of cucurbitacin-containing phloem latex from cuts. Therefore, it can be hypothesized that, analogous to laticifers, EFP sieve tube occlusion also is only effective after pressure release by exudation and is necessary for reloading the EFP's defensive arsenal. Systemic polysaccharide accumulation induced by leaf wounding did not prevent pressure-driven exudation but rather might function in clogging of an insect's mouth parts. Accordingly, sticky compounds in phloem latex, which accumulated after leaf wounding but were present also in control samples, effectively plugged pipette tips during the sampling procedure.

Stress-Induced Energy Metabolism in the Phloem Is Controlled by SNF1-Related Kinases and a 32-kD 14-3-3 Protein and Is Not Limited by Oxygen Availability

Phloem is largely isolated from air oxygen by many layers of surrounding cells. Using microelectrodes, the oxygen tension was determined to be 15% at the epidermis but only 5% to 6% in the phloem region of castor bean stems (van Dongen et al., 2003). Exposure of stem tissue to 21%, 10%, and 5% oxygen caused a gradual decline in ATP levels of phloem samples, indicative for oxygen limitation of energy metabolism in the fascicular phloem under natural conditions (van Dongen et al., 2003). Geigenberger (2003) proposed that under stress conditions, a rise in mitochondrial oxygen-consuming respiration would cause hypoxia or even anoxia and, consequently, energy deficiency in the phloem. Accordingly, in phloem exudates from castor bean stem sections, which were incubated in zero-oxygen atmosphere for 90 min, ATP dropped to 50% of the ambient air control (van Dongen et al., 2003). As a consequence, energy-dependent Suc transport was inhibited and other markers of energy metabolism such as pyruvate, Glc-6-P, citrate, and malate were also diminished, whereas lactate and ethanol levels increased under severe oxygen deficiency.

However, in the EFP of pumpkin plants, the energy status as determined by ATP levels did not change strongly in response to stress. After an initial insignificant depression, ATP concentrations even increased by about 17% at 6 to 24 h upon wounding. ATP was most likely derived from enhanced glycolysis and the citrate cycle, because Suc, Glc-6-P, pyruvate, as well as the citrate cycle intermediates citrate, malate, and phosphate were strongly elevated after wounding. The intermediates of the citrate cycle displayed very similar kinetics, with an early rise at 3 h and a decline toward control levels at 24 h after leaf damage. Lactate was not consistently regulated, indicating that, in contrast to oxygen-deficient fascicular phloem of castor bean, fermentation of pyruvate is not an essential pathway for energy production in the stressed EFP. Collectively, these results imply that either stress does not cause hypoxia in the EFP or the energy-consuming stress response is at least not limited by oxygen availability. In comparison with the fascicular phloem, the EFP consists of a network of sieve elements (Turgeon and Oparka, 2010) connecting well-oxygenated outer tissues with oxygen-deficient inner tissues. Hence, the EFP is probably better supplied with oxygen than the fascicular phloem. It would be interesting to learn if the EFP even plays a role in "ventilation" of the fascicular phloem and other internal tissues.

Glc-6-P and Fru-6-P are central metabolites at the interface between glycolysis and gluconeogenesis and are involved in nucleotide sugar metabolism and cell wall synthesis (Seifert, 2004; Schluepmann et al., 2012). Immediately after wounding, Glc-6-P was probably used for callose formation, since polysaccharides strongly accumulated at the 0.5- to 3-h time points (Fig. 2B). From 3 h on, EFP metabolism switched toward increased energy supply. The observed accumulation of Glc-6-P at 3 h after wounding could originate from different sources, including (1) digestion of Suc or other carbohydrates in the course of glycolysis, (2) breakdown of callose/polysaccharides after transient partial sieve tube occlusion, or (3) either/both of these two sources in conjunction with inhibition of Glc-6-P-consuming pathways. Our results provide evidence for a tightly controlled channeling of Glc-6-P into glycolysis and the citrate cycle (Supplemental Fig. S4), because intermediates of the citrate cycle increased with similar kinetics like Glc-6-P. One metabolic checkpoint seems to be Glc-6-P dehydrogenase, which is the first enzyme of the oxidative pentose phosphate pathway. This pathway mainly provides reducing power in the form of NADPH for metabolic processes but not the energy equivalents NADH and ATP. Glc-6-P dehydrogenase was strongly inhibited at 3 and 24 h after leaf wounding, suggesting that the pentose phosphate pathway is down-regulated under high energy demand.

Cell wall synthesis consumes most of the carbon in plant cells, main components being the nucleotide sugars Glc-6-P, Glc-1-P, UDP-Glc, and GDP-L-Fuc (Seifert, 2004). In wound-induced stress conditions, the EFP down-regulated the cell wall-synthesizing enzymes GDP-L-Fuc synthase and UDP-L-Rha synthase (Supplemental Fig. S4). As mentioned above, callose synthase is probably also inactivated after transient sieve tube occlusion. If the same applies for cellulose synthase remains to be answered in a future study. Moreover, the cell wall component Hyp, which is used for the synthesis of Hyp-rich glycoproteins, and myo-inositol declined in phloem latex from wounded plants. Inhibition of myoinositol synthesis could also contribute to the accumulation of its precursor Suc. The latter disaccharide is probably both a substrate for glycolysis as well as a product of gluconeogenesis. Alternatively, increased Suc levels could indicate enhanced phloem transport/sugar uptake (van Dongen et al., 2003). Amino acids accumulate late, suggesting that in the early phase of the stress response energy metabolism is preferred and, later, energy and carbon are used for amino acid and protein synthesis. Collectively, these results demonstrate that a major part of the EFP stress response is dedicated to metabolic reprogramming toward an increase in energy production by enhanced glycolysis and the citrate cycle.

SNF1-Related Protein Kinases and the 14-3-3 32-kD Endonuclease

The two SNF1-related protein kinases SnRK1 and SnRK2 are currently emerging as central regulators of energy and carbon metabolism under stress conditions (Boudsocq and Laurière, 2005; Polge and Thomas, 2007; Baena-González and Sheen, 2008). Sugar or energy depletion during hypoxia, long darkness, and phosphate starvation were shown to activate SnRK1, which then

triggered the degradation of alternative energy sources such as Suc, starch, cell wall compounds, amino acids, and storage lipids (Baena-González et al., 2007; Lee et al., 2009; Bailey-Serres et al., 2012; Schluepmann et al., 2012). Accordingly, overexpression of the Arabidopsis (*Arabidopsis thaliana*) SnRK1 subunit KIN10 induced the expression of genes related to catabolism, but genes related to energy-consuming processes and anabolism were repressed (Baena-González et al., 2007). Exogenously supplied Suc was more efficiently used for energy production by KIN10-silenced plants as compared with KIN10 overexpressors (Baena-González et al., 2007). Based on these findings, the observed wound-induced reduction of SnRK1 protein levels in phloem latex would provoke a rise in energy metabolism in the course of the EFP stress response. Basal levels of SnRK1 in control samples might fine-tune the energy economy by establishing a low metabolic rate at rest.

In line with this hypothesis, the SnRK1 subunit GAL83 of *Nicotiana attenuata* was down-regulated in gene expression after leaf wounding, which was associated with the allocation of carbohydrates from leaves to the roots for improved herbivore tolerance (Schwachtje et al., 2006). Moreover, Coello et al. (2012) found a drastic decline in SnRK1 levels at 6 to 10 h after abscisic acid (ABA) treatment of wheat (*Triticum aestivum*) roots, but the total SnRK1 activity was weakly enhanced due to a simultaneous ABA-induced increase in phosphorylation/activation. If the wound-induced down-regulation of SnRK1 in the EFP is mediated by the well-known wound signal ABA remains to be investigated. Notably, SnRK1 activity is allosterically inhibited by Glc-6-P (Toroser et al., 2000). Given the strong down-regulation of SnRK1 protein abundance and the accumulation of inhibitory levels of Glc-6-P in phloem latex, it can be assumed that SnRK1 activity is reduced in the EFP after leaf wounding.

In phloem latex, the 14-3-3 32-kD endonuclease was induced at 3 and 24 h after leaf wounding. 14-3-3 proteins interact with phosphorylated target proteins, thereby modulating their conformation and/or activity. Originally, they were thought to mainly regulate metabolic enzymes (Huber et al., 2002) but are now recognized as central mediators of signal transduction (Gökirmak et al., 2010; Jaspert et al., 2011). The EFP 14-3-3 32-kD endonuclease is highly similar to potato (*Solanum tuberosum*) 14-3-3 proteins (Aksamit et al., 2005; Zuk et al., 2005). In the context of phloem signaling, it is of particular interest that expression of the potato 14-3-3 16R and 20R isoforms is restricted mainly to vascular tissues and adjacent parenchyma cells (Aksamit et al., 2005). Both 14-3-3-coding genes were inducible by ABA, which was mediated by promoters containing Myc-binding sites, but were differentially expressed in response to various abiotic stresses and phytohormones (Aksamit et al., 2005).

The promoter of the 14-3-3 isoform 16R was inducible by Suc. Moreover, transgenic potato plants silenced in 14-3-3 genes displayed reduced nitrate reductase, Suc phosphate synthase, and Suc synthase activities accompanied by increases in starch, Suc, and protein levels (Zuk et al., 2005). This phenotype could be complemented by overexpressing the 14-3-3 32-kD endonuclease from zucchini (*Cucurbita pepo*). In *Hevea brasiliensis* latex, 14-3-3 proved to be inducible by JA, corroborating a possible role of this protein in defense responses (Yang et al., 2012). Thus, 14-3-3 proteins might, like SnRKs, act as integrators of carbohydrate, energy, and (ABA- or JA-controlled) stress metabolism. If the 14-3-3 endonuclease and SnRK1/2 are antagonists in the same signaling pathways will be deciphered in future studies.

JA Signaling and the Accumulation of Defense-Related Proteins during Systemic Wound Responses of the EFP

Leaf damage simulating herbivore attack triggers systemic signaling cascades in plants, and JA derivatives were hypothesized to act as phloem-mobile signals in the systemic wound response (Li et al., 2002; Ryan and Moura, 2002; Koo and Howe, 2009; Sun et al., 2011; Gaupels and Vlot, 2012). Accordingly, wounding triggered JA synthesis in the tomato (*Solanum lycopersicum*) sieve elements (Hause et al., 2000, 2003), and isotope-labeled JA was found to be systemically transported in the sieve tubes (Zhang and Baldwin, 1997; Thorpe et al., 2007). However, to date, few data are available on the actual concentrations of this hormone in phloem exudates. We measured the JA and JA-Ile contents in phloem latex from wounded pumpkin. Jasmonates were not detectable in samples from untreated plants but accumulated rapidly at 0.5, 1, and 3 h after wounding. Maximum concentrations were measured at the 1-h time point, when JA and JA-Ile reached 107 and 49 nM, respectively. The kinetics is very similar to previously reported jasmonate accumulation in wounded and systemic leaves of tomato and is indicative for the induction of a systemic wound response (Koo et al., 2009). Interestingly, declining jasmonate levels at 3 h after leaf damage coincided with the down-regulation of two proteins of the COP9 signalosome, which is required for the expression of JA biosynthesis-related genes (Feng et al., 2003).

In the EFP, jasmonates could elicit the local accumulation of defense-related proteins such as SLW1. *SLW1* was expressed in response to infestation of squash with the phloem-feeding silverleaf whitefly and upon treatment with methyl jasmonate but not wounding (van de Ven et al., 2000). The most prominent wound-induced protein in pumpkin phloem latex was identified by ICPL, SDS-PAGE, LC-MS, and western-blot analyses to be an 18-kD cyclophilin. CYP18 is highly similar to Arabidopsis ROC1/AtCYP18-3, which was shown to be 3.5-fold induced in expression by wounding (Chou and Gasser, 1997). We used anti-AtCYP18-3 antibodies for the detection of CYP18 in phloem latex. Previously, these antibodies were applied for demonstrating the presence of cyclophilins in phloem latex from pumpkin as well as phloem exudates from six monocotyledonous and

dicotyledonous plant species, including castor bean (Schobert et al., 1998; Gottschalk et al., 2008). Hence, 18-kD cyclophilins are conserved constituents of EFP as well as fascicular phloem and probably fulfill essential functions in the phloem. In castor bean, phloem cyclophilin displayed high peptidyl-prolyl cis-trans-isomerase activity, interacted with plasmodesmata, and trafficked from cell to cell (Gottschalk et al., 2008). Based on these findings, phloem cyclophilins may act as molecular chaperones modulating the import, mobility, and function of target proteins in the phloem.

Further wound-elicited chaperones, such as HSP81 and Chaperonin-Containing Complex Protein1, could have similar functions in the EFP. PP16-1 is yet another protein in phloem latex related to transport and signaling. The protein is a paralog to a movement protein of the *Red clover necrotic mosaic virus* and acts as mRNA carrier within the phloem of pumpkin (Xoconostle-Cázares et al., 1999). Aoki et al. (2005) uncovered destination-selective transport of PP16-1 and PP16-2 against the mass flow from shoot to roots of rice. To date, no further details about the role of PP16-1 in stress signaling processes are known. However, PP16-1 is regulated with similar kinetics to CYP18, suggesting common upstream signals or even a functional link between both proteins.

Protein kinases, particularly MAPKs, are often activated by phosphorylation in the course of kinase signaling cascades. However, some kinases, including MAPKs, were also found to be regulated in gene expression after stress treatments (Mizoguchi et al., 1996). In pumpkin phloem latex, the three protein kinases cyclin-dependent kinase A, NO_3^- stress-induced MAPK, and MAPK6 were increased in protein levels at 24 h after leaf wounding. Supportive of these results, CDC2a, a cyclin-dependent kinase A of Arabidopsis, was strongly induced at the transcriptional level by wounding (Hemerly et al., 1993). In cucumber plants, the NO_3^- stress-induced MAPK was also inducible by root infection with *Trichoderma asperellum*. A more detailed characterization revealed that this cucumber MAPK is highly homologous to the tobacco wound-induced protein kinase, and gene expression was actually inducible within 10 min in the wounded leaves and after 24 but not 3 h in systemic leaves (Shoresh et al., 2006). Similarly, the NO_3^-/*T. asperellum*-induced MAPK in the EFP accumulated at 24 h but not 3 h after leaf wounding. It was recently reported that MAPK6 is an important component of the JA signaling pathway in Arabidopsis (Takahashi et al., 2007). If the regulation of MAPK6 in the EFP is linked to JA signaling is not yet known.

Indications for Redox Signaling in the Phloem

Recently, a microscopic study using the nitric oxide (NO)-sensitive dye diaminofluorescein revealed interaction of the redox signals hydrogen peroxide and NO in the phloem (Gaupels et al., 2008b). Hydrogen peroxide applied to the bare-lying phloem of *Vicia faba* elicited rapid NO synthesis in companion cells, whereas watering of pumpkin with hydrogen peroxide induced NO-dependent Tyr nitration of proteins in the EFP. A further hint toward redox signaling in the EFP could be the increase in MAPK6 levels upon leaf wounding, as reported in this study. The Arabidopsis homolog of this enzyme was shown to mediate the hydrogen peroxide-stimulated production of NO in lateral root formation (Wang et al., 2010).

PP1 and PP2 are well-known redox sensors in phloem latex. They were shown to interact via the formation of intermolecular disulfide bridges between Cys residues (Read and Northcote, 1983). Under oxidizing conditions, extensive polymerization turns PP1/PP2 complexes insoluble, causing gelation of EFP exudates (Read and Northcote, 1983). In the air, this process takes several hours, but if exudates are diluted in neutral or alkaline buffers, Cys residues get exposed, facilitating oxidation and consequently sample gelation within minutes (Alosi et al., 1988). After leaf wounding, we observed a delay in sample gelation at 6 to 48 h, which could reflect redox modifications of PP1/PP2 during the wound response.

Therefore, oxidation/carbonylation of phloem proteins was investigated by anti-dinitrophenol (DNP) western-blot analyses. By this method, the carbonylated proteins PP16-1, CYP18, and two isoforms of PP2 were immunodetected. Notably, PP1 was not carbonylated. In contrast, PP2 was strongly carbonylated even in EFP exudates from untreated control plants, suggesting that PP2 is oxidized under nonstress conditions. At 6-, 12-, and 24-h time points, PP2 signal intensity decreased, but it increased again at 48 and 96 h after wounding. This decline in carbonylation

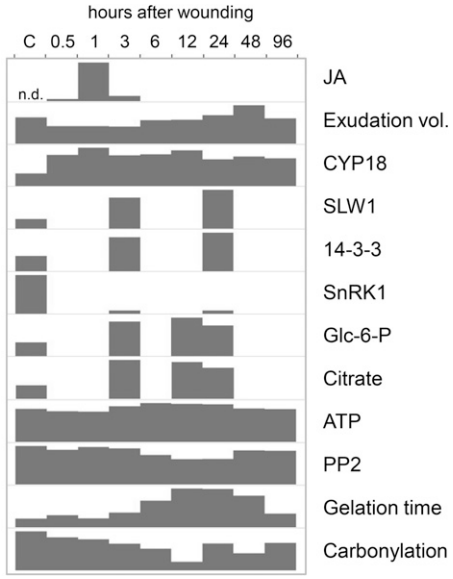

Figure 9. Summary of main results. Responses of the pumpkin EFP to leaf wounding are shown. Glc-6-P and citrate are given in relative signal intensity ratios (only one representative replicate is shown). For all other parameters, the height of the bars is proportional to control levels. Carbonylation is visualized by ImageJ quantification of the anti-DNP western blot. C, Control; n.d., not detected.

correlated well with the observed delay in sample gelling at 6 to 48 h (Fig. 9), suggesting that the increase in the reduction of PP2 hinders oxidation-dependent polymerization of PP2/PP1. The decrease in carbonylation of PP2 but not CYP18 and PP16-1 after wounding could be explained by enhanced turnover of oxidized PP2, the activity of antioxidant enzymes interacting specifically with PP2, or a redox-dependent change in conformation of PP2 potentially hiding amino acids that are prone to carbonylation.

Decreased carbonylation could even be involved in the observed decline in PP2 levels in response to leaf wounding, which could be caused by redox-regulated protein mobilization in the phloem in the course of signaling or defense events. It was proposed previously that PP2 might then occlude sieve plates (Furch et al., 2010). However, the data presented here do not support this hypothesis, because transient sieve tube occlusion occurs earlier than the reduction in PP2 levels (Fig. 9). Alternatively, PP2, PP1, and callose might cover the wounded tissue to protect the plant from insect and pathogen ingress. In this model, the lectin PP2 would interfere in an unknown mode with surface or internal GlcNAc of the attackers, while the filamentous PP1 in conjunction with callose could clog the mouth parts of insects or affect the motility of pathogens (Read and Northcote, 1983; Beneteau et al., 2010; Konno, 2011). PP2 was also identified as an RNA-transporting protein in melon (*Cucumis melo*) EFP, and as a lectin it showed affinity for phloem-internal glycoproteins (Gomez et al., 2005; Beneteau et al., 2010). Neither RNAs nor glycoproteins carried by PP2 could be identified to date. Thus, the functions of PP1 and PP2 in stress defense or signaling remain ambiguous.

CONCLUSION

This study was aimed at deciphering responses of the EFP to leaf wounding by metabolomic and proteomic approaches. As summarized in Figure 9, the EFP launched within 3 h a systemic wound response including JA accumulation, partial sieve tube occlusion, a rise in defensive protein levels, and adaptation of carbon metabolism to the higher energy demand. Later wounding caused a decline in the oxidation of PP2, which correlated with a decrease in PP2 protein level and a delay in redox-dependent sample gelation. Some of our findings for the EFP could apply also to the fascicular phloem. For instance, the major phloem proteins CYP18 and PP2 might be valuable markers for stress responses and redox signaling in both phloem systems.

MATERIALS AND METHODS

Plant Material, Sampling, and Sample Gelation Assay

Leaf edges of 4- to 5-week-old pumpkin plants (*Cucurbita maxima* 'Gele Centenaar') grown under greenhouse conditions were crushed between the lids of two 50-mL polypropylene reaction tubes. Phloem samples were collected in the greenhouse as follows. Petioles and stems were cut using a razor blade, and the basal side of the cut was immediately blotted with Kimtech Science paper (Kimberly-Clark) to remove the content of damaged nonvascular cells and fascicular phloem sap. Exuding phloem latex was subsequently collected by a micropipette for less than 2 min. Control plants were left untreated. Pumpkin phloem latex was either snap frozen in liquid N_2 for metabolite analyses or mixed with the same volume of phloem buffer if not otherwise stated (50 mM Tris-HCl, pH 7.8, 0.1% β-mercaptoethanol; McEuen and Hill, 1982). Aphid stylectomy was used for phloem sampling according to Gaupels et al. (2008a, 2008c) with the aphid *Macrosiphum euphorbiae*. The time until sample gelation was measured after the addition of 3 volumes of alkaline buffer (25 mM HEPES/NaOH, pH 7.8) to the phloem latex (80 μL). Samples were assumed to be gelated when they could not be mixed by vortexing anymore.

Jasmonate Measurements

JA and JA-Ile in 1 mL of phloem latex from seven to 10 plants were determined as described by Hause et al. (2000).

ATP Assay

Five microliters of phloem latex was frozen in liquid nitrogen and stored at −80°C. Immediately before the measurements, 5 μL of phloem buffer and 40 μL of water were added, and ATP was determined using the ATP Bioluminescence Assay Kit CLSII (Roche) according to the manufacturer's instructions.

Metabolomics

GC-Time of Flight-MS

The sample extraction process involved the use of a single-phase solvent (chloroform-methanol-water) that was optimized for recovery of a wide range of metabolites (Beckmann et al., 2007). Metabolites were extracted by mixing 9 μL of phloem latex with 81 μL of chilled $CHCl_3$:methanol:water (1:2.5:1, v/v/v), and samples were stored at −18°C. After the addition of 90 μL of chilled methanol, samples were centrifuged (18,000*g* for 3 min at 0°C), and the resulting supernatant was dried in vacuo. GC-time of flight-MS analysis was performed as described previously (Catchpole et al., 2005; Beckmann et al., 2007) using tetramethylsilane derivatization and a Pegasus III GC-time of flight-MS system (Leco; http://www.leco.com/) fitted with a 20 m DB5 MS column. Peak finding and peak deconvolution were performed using ChromaTof software (Leco). Mass spectra of all detected compounds were compared with spectra in the National Institute of Standards and Technology library and with in-house and publicly available databases. Targeted peak lists were generated, and the peak apex intensity of a characteristic mass in a retention time window for each GC-MS data set (using Matlab; The Mathworks) was saved in the form of an intensity matrix (run × metabolite) for further statistical analysis.

Data Analysis

Due to the three-dimensional data structure, peak aligned and $\log_{10}$-transformed GC-MS intensity data were first filtered by univariate data analysis using ANOVA (function ANOVA1 in Matlab; The Mathworks) to reduce their size. Metabolite signals with ANOVA $P > 5 \times 10^{-4}$ were removed from each data set. The main criterion for good model selection (i.e. discriminatory metabolites) in multidimensional GC-MS metabolomics data sets is $P < 1 \times 10^{-10}$ (ANOVA). However, a P value threshold of 1×10^{-6} is acceptable, considering a false discovery rate level of 0.001. In the second step, 80 metabolites, including all unique metabolites showing significant differences between treatment groups (n = 10 biological replicates for each group and experiment), were targeted in the three GC-MS raw data sets of replicated experiments. ANOVA was performed on $\log_{10}$-transformed and normalized data. Results are shown for metabolites that were significantly regulated ($P <$ 0.05) in at least two of three experiments.

HPLC and FIE-MS

Metabolites of 120 μL of phloem latex were extracted by mixing with 180 μL of chilled $CHCl_3$:methanol:water (1:2.5:1, v/v/v), and samples were stored at −18°C. After the addition of 300 μL of chilled methanol, samples

were centrifuged (18,000*g* for 3 min at 0°C), the resulting supernatant was dried in vacuo, and the metabolites were redissolved in 60 μL of 0.1% trifluoroacetic acid (TFA)/60% methanol. A Dionex HPLC system consisting of an Automated Sample Injector (ASI 100), P580 pump, column oven, and PDA-100 photodiode array detector was controlled by Chromeleon version 6.5 software. Ten microliters was injected onto a CC 250 × 4.6 Nucleodur C18 Gravity 5-μm column (Macherey-Nagel). A binary gradient (mobile phase A, water and 0.1% TFA; mobile phase B, methanol and 0.1% TFA) from 0% B (held for 2 min) to 100% B (held for 6 min) within 10 min followed by a 10-min equilibration period at 0% B was used to separate metabolites. A flow of 1 mL min^{-1} was maintained at 40°C. HPLC fractions containing the peak that eluted from 8 to 10 min of elution time were collected and analyzed by FEI-MS as described (Parker et al., 2009). FIE-MS and MS experiments were performed on a linear ion trap (LTQ; Thermo).

Proteomics

ProteoMiner Treatment and ICPL

A 120-μL pumpkin phloem exudate (25 mg protein mL^{-1}) was mixed with the same volume of phloem buffer. Redox-sensitive Cys residues of PP1/PP2 were alkylated by adding 25 mM (final concentration) iodoacetamide. Afterward, β-mercaptoethanol and iodoacetamide were removed by gel filtration, and proteins were collected in 120 μL of phloem buffer without β-mercaptoethanol. ProteoMiner beads were applied according to the manual. Final protein amount was 3 mg at a concentration of 25 mg mL^{-1}. After washing, proteins were eluted from beads by twice applying 50 μL of commercial 4× Laemmli buffer (Roth) at 95°C. Proteins were precipitated using the 2D Clean-up Kit (GE Healthcare) and dissolved in 40 μL of 100 mM HEPES, pH 8.5. Stable isotope labeling of the phloem proteins was done with the ICPL Triplex Kit (Serva) according to the manual with doubled volumes of all kit reagents. For each triplicate, isotope-labeled phloem proteins from control and wounded plants, time points 3 and 24 h after wounding, were combined. Proteins were again precipitated using the 2D Clean-up Kit and separated by SDS-PAGE. The gel was cut in six pieces per sample and analyzed by LC-MS/MS.

MS Analysis and Data Processing

After Coomassie blue staining, gel slices from one-dimensional ICPL gels were excised and subjected to in-gel digestion before MS analysis. Digested peptides were analyzed by nano-HPLC (Ultimate 3000; Dionex) coupled to a linear quadrupole ion trap-Orbitrap (LTQ Orbitrap XL) mass spectrometer (Thermo Fisher) equipped with a nano-electrospray ionization source. A nonlinear gradient using 2% acetonitrile in 0.1% formic acid in water (A) and 0.1% formic acid in 98% acetonitrile (B) was used with a flow rate of 300 nL min^{-1}. The mass spectrometer was operated in the data-dependent mode to automatically switch between Orbitrap-MS and LTQ-MS/MS. General MS conditions were as follows: ion selection threshold was 500 counts for MS/MS, an activation default instrument setting in Q text box of 0.25, and activation time of 30 ms was also applied for MS/MS. The MS/MS spectra were searched against a customized database (Fröhlich et al., 2012) by using MASCOT (version 2.3.02; Matrix Science) with the following parameters: a precursor mass error tolerance of 10 ppm and a fragment tolerance of 0.6 D. One missed cleavage was allowed. Carbamidomethylation was set as a fixed modification. Oxidized Met and ICPL_0, ICPL_4, and ICPL_6 for Lys were set as variable modifications.

Data processing for the identification and quantitation of ICPL-labeled protein triplex pairs was performed using Proteome Discoverer version 1.3 (Thermo Fisher) as described in Supplemental Information S1. Proteins with ratios of heavy/light label greater or less than 1.6-fold change were defined as being differentially expressed ($P < 0.05$; Perseus statistical tool). Proteins identified by at least two unique constituent peptides in at least two of the three biological replicates were taken into consideration.

SDS-PAGE and Western-Blot Analyses

SDS-PAGE, Coomassie blue staining, and silver staining were performed according to Gaupels et al. (2008b, 2008c). ImageJ was applied for the quantification of SDS-PAGE bands. The generation and application of anti-CYP18-3 was described previously (Lippuner et al., 1994). Anti-OsSnRK1A/B antiserum was raised against the synthetic peptide N′-RKWALGLQSRAHPRE-C′, which represents amino acid residues 383 to 397 of rice (*Oryza sativa*) SnRK1A and SnRK1B. The antibodies were a generous gift of Su-May Yu and Kuo-Wei Lee (Institute of Molecular Biology, Academia Sinica). The OxyBlot Protein Oxidation Detection Kit (Millipore) was employed for the detection of carbonylated proteins in 2.5 μL of phloem latex/2.5 μL of phloem buffer following the manufacturer's instructions.

Supplemental Data

The following materials are available in the online version of this article.

Supplemental Figure S1. Lactate levels in phloem latex.

Supplemental Figure S2. Amino acids and primary amines.

Supplemental Figure S3. ProteoMiner effect.

Supplemental Figure S4. Regulation of carbohydrate and energy metabolism after wounding.

Supplemental Table S1. Labeled and identified phloem latex proteins.

ACKNOWLEDGMENTS

We thank Charles Gasser for providing the anti-CYP18-3 antibodies, Su-May Yu and Kuo-Wei Lee for providing the anti-OsSnRK1A/B antibodies, Ray Smith and Tom Thomas for plant management, and Rob Darby for support in the metabolomics project.

Received August 10, 2012; accepted October 18, 2012; published October 19, 2012.

LITERATURE CITED

Aksamit A, Korobczak A, Skala J, Lukaszewicz M, Szopa J (2005) The 14-3-3 gene expression specificity in response to stress is promoter-dependent. Plant Cell Physiol **46:** 1635–1645

Alosi MC, Melroy DL, Park RB (1988) The regulation of gelation of phloem exudate from *Cucurbita* fruit by dilution, glutathione, and glutathione reductase. Plant Physiol **86:** 1089–1094

Aoki K, Suzui N, Fujimaki S, Dohmae N, Yonekura-Sakakibara K, Fujiwara T, Hayashi H, Yamaya T, Sakakibara H (2005) Destination-selective long-distance movement of phloem proteins. Plant Cell **17:** 1801–1814

Atkins CA, Smith PM, Rodriguez-Medina C (2011) Macromolecules in phloem exudates: a review. Protoplasma **248:** 165–172

Baena-González E, Rolland F, Thevelein JM, Sheen J (2007) A central integrator of transcription networks in plant stress and energy signalling. Nature **448:** 938–942

Baena-González E, Sheen J (2008) Convergent energy and stress signaling. Trends Plant Sci **13:** 474–482

Bailey-Serres J, Fukao T, Gibbs DJ, Holdsworth MJ, Lee SC, Licausi F, Perata P, Voesenek LA, van Dongen JT (2012) Making sense of low oxygen sensing. Trends Plant Sci **17:** 129–138

Beckmann M, Enot DP, Overy DP, Draper J (2007) Representation, comparison, and interpretation of metabolome fingerprint data for total composition analysis and quality trait investigation in potato cultivars. J Agric Food Chem **55:** 3444–3451

Beneteau J, Renard D, Marché L, Douville E, Lavenant L, Rahbé Y, Dupont D, Vilaine F, Dinant S (2010) Binding properties of the *N*-acetylglucosamine and high-mannose *N*-glycan PP2-A1 phloem lectin in Arabidopsis. Plant Physiol **153:** 1345–1361

Boudsocq M, Laurière C (2005) Osmotic signaling in plants: multiple pathways mediated by emerging kinase families. Plant Physiol **138:** 1185–1194

Buhtz A, Kolasa A, Arlt K, Walz C, Kehr J (2004) Xylem sap protein composition is conserved among different plant species. Planta **219:** 610–618

Carroll CR, Hoffman CA (1980) Chemical feeding deterrent mobilized in response to insect herbivory and counteradaptation by *Epilachna tredecimnotata*. Science **209:** 414–416

Catchpole GS, Beckmann M, Enot DP, Mondhe M, Zywicki B, Taylor J, Hardy N, Smith A, King RD, Kell DB, et al (2005) Hierarchical metabolomics demonstrates substantial compositional similarity between

genetically modified and conventional potato crops. Proc Natl Acad Sci USA **102:** 14458–14462

Chou IT, Gasser CS (1997) Characterization of the cyclophilin gene family of *Arabidopsis thaliana* and phylogenetic analysis of known cyclophilin proteins. Plant Mol Biol **35:** 873–892

Coello P, Hirano E, Hey SJ, Muttucumaru N, Martinez-Barajas E, Parry MA, Halford NG (2012) Evidence that abscisic acid promotes degradation of SNF1-related protein kinase (SnRK) 1 in wheat and activation of a putative calcium-dependent SnRK2. J Exp Bot **63:** 913–924

Feng S, Ma L, Wang X, Xie D, Dinesh-Kumar SP, Wei N, Deng XW (2003) The COP9 signalosome interacts physically with SCF COI1 and modulates jasmonate responses. Plant Cell **15:** 1083–1094

Fröhlich A, Gaupels F, Sarioglu H, Holzmeister C, Spannagl M, Durner J, Lindermayr C (2012) Looking deep inside: detection of low-abundance proteins in leaf extracts of Arabidopsis and phloem exudates of pumpkin. Plant Physiol **159:** 902–914

Fröhlich A, Lindermayr C (2011) Deep insights into the plant proteome by pretreatment with combinatorial hexapeptide ligand libraries. J Proteomics **74:** 1182–1189

Furch AC, Zimmermann MR, Will T, Hafke JB, van Bel AJ (2010) Remote-controlled stop of phloem mass flow by biphasic occlusion in *Cucurbita maxima*. J Exp Bot **61:** 3697–3708

Gaupels F, Buhtz A, Knauer T, Deshmukh S, Waller F, van Bel AJ, Kogel KH, Kehr J (2008a) Adaptation of aphid stylectomy for analyses of proteins and mRNAs in barley phloem sap. J Exp Bot **59:** 3297–3306

Gaupels F, Furch AC, Will T, Mur LA, Kogel KH, van Bel AJ (2008b) Nitric oxide generation in *Vicia faba* phloem cells reveals them to be sensitive detectors as well as possible systemic transducers of stress signals. New Phytol **178:** 634–646

Gaupels F, Knauer T, van Bel AJ (2008c) A combinatory approach for analysis of protein sets in barley sieve-tube samples using EDTA-facilitated exudation and aphid stylectomy. J Plant Physiol **165:** 95–103

Gaupels F, Vlot AC (2012) Plant defense and long-distance signaling in the phloem. *In* GA Thompson, AJE van Bel, eds, Phloem: Molecular Cell Biology, Systemic Communication, Biotic Interactions, Vol 1. Wiley-Blackwell, Hoboken, NJ, pp 227–247

Geigenberger P (2003) Response of plant metabolism to too little oxygen. Curr Opin Plant Biol **6:** 247–256

Gökirmak T, Paul AL, Ferl RJ (2010) Plant phosphopeptide-binding proteins as signaling mediators. Curr Opin Plant Biol **13:** 527–532

Gomez G, Torres H, Pallas V (2005) Identification of translocatable RNA-binding phloem proteins from melon, potential components of the long-distance RNA transport system. Plant J **41:** 107–116

Gottschalk M, Dolgener E, Xoconostle-Cázares B, Lucas WJ, Komor E, Schobert C (2008) *Ricinus communis* cyclophilin: functional characterisation of a sieve tube protein involved in protein folding. Planta **228:** 687–700

Hagel JM, Yeung EC, Facchini PJ (2008) Got milk? The secret life of laticifers. Trends Plant Sci **13:** 631–639

Hause B, Hause G, Kutter C, Miersch O, Wasternack C (2003) Enzymes of jasmonate biosynthesis occur in tomato sieve elements. Plant Cell Physiol **44:** 643–648

Hause B, Stenzel I, Miersch O, Maucher H, Kramell R, Ziegler J, Wasternack C (2000) Tissue-specific oxylipin signature of tomato flowers: allene oxide cyclase is highly expressed in distinct flower organs and vascular bundles. Plant J **24:** 113–126

Hemerly AS, Ferreira P, de Almeida Engler J, Van Montagu M, Engler G, Inzé D (1993) cdc2a expression in *Arabidopsis* is linked with competence for cell division. Plant Cell **5:** 1711–1723

Huber SC, MacKintosh C, Kaiser WM (2002) Metabolic enzymes as targets for 14-3-3 proteins. Plant Mol Biol **50:** 1053–1063

Jaspert N, Throm C, Oecking C (2011) Arabidopsis 14-3-3 proteins: fascinating and less fascinating aspects. Front Plant Sci **2:** 96

Konno K (2011) Plant latex and other exudates as plant defense systems: roles of various defense chemicals and proteins contained therein. Phytochemistry **72:** 1510–1530

Koo AJ, Gao X, Jones AD, Howe GA (2009) A rapid wound signal activates the systemic synthesis of bioactive jasmonates in Arabidopsis. Plant J **59:** 974–986

Koo AJ, Howe GA (2009) The wound hormone jasmonate. Phytochemistry **70:** 1571–1580

Lee KW, Chen PW, Lu CA, Chen S, Ho TH, Yu SM (2009) Coordinated responses to oxygen and sugar deficiency allow rice seedlings to tolerate flooding. Sci Signal **2:** ra61

Li L, Li C, Lee GI, Howe GA (2002) Distinct roles for jasmonate synthesis and action in the systemic wound response of tomato. Proc Natl Acad Sci USA **99:** 6416–6421

Lin MK, Lee YJ, Lough TJ, Phinney BS, Lucas WJ (2009) Analysis of the pumpkin phloem proteome provides insights into angiosperm sieve tube function. Mol Cell Proteomics **8:** 343–356

Lippuner V, Chou IT, Scott SV, Ettinger WF, Theg SM, Gasser CS (1994) Cloning and characterization of chloroplast and cytosolic forms of cyclophilin from *Arabidopsis thaliana*. J Biol Chem **269:** 7863–7868

Malter D, Wolf S (2011) Melon phloem-sap proteome: developmental control and response to viral infection. Protoplasma **248:** 217–224

McEuen AR, Hill HAO (1982) Superoxide, hydrogen peroxide, and the gelling of phloem sap from *Cucurbita pepo*. Planta **154:** 295–297

Mizoguchi T, Irie K, Hirayama T, Hayashida N, Yamaguchi-Shinozaki K, Matsumoto K, Shinozaki K (1996) A gene encoding a mitogen-activated protein kinase kinase kinase is induced simultaneously with genes for a mitogen-activated protein kinase and an S6 ribosomal protein kinase by touch, cold, and water stress in *Arabidopsis thaliana*. Proc Natl Acad Sci USA **93:** 765–769

Mullendore DL, Windt CW, Van As H, Knoblauch M (2010) Sieve tube geometry in relation to phloem flow. Plant Cell **22:** 579–593

Parker D, Beckmann M, Zubair H, Enot DP, Caracuel-Rios Z, Overy DP, Snowdon S, Talbot NJ, Draper J (2009) Metabolomic analysis reveals a common pattern of metabolic re-programming during invasion of three host plant species by *Magnaporthe grisea*. Plant J **59:** 723–737

Polge C, Thomas M (2007) SNF1/AMPK/SnRK1 kinases, global regulators at the heart of energy control? Trends Plant Sci **12:** 20–28

Read SM, Northcote DH (1983) Chemical and immunological similarities between the phloem proteins of three genera of the Cucurbitaceae. Planta **158:** 119–127

Ryan CA, Moura DS (2002) Systemic wound signaling in plants: a new perception. Proc Natl Acad Sci USA **99:** 6519–6520

Schluepmann H, Berke L, Sanchez-Perez GF (2012) Metabolism control over growth: a case for trehalose-6-phosphate in plants. J Exp Bot **63:** 3379–3390

Schobert C, Baker L, Szederkenyi J, Grossmann P, Komor E, Hayashi H, Chino M, Lucas WJ (1998) Identification of immunologically related proteins in sieve-tube exudate collected from monocotyledonous and dicotyledonous plants. Planta **206:** 245–252

Schwachtje J, Minchin PE, Jahnke S, van Dongen JT, Schittko U, Baldwin IT (2006) SNF1-related kinases allow plants to tolerate herbivory by allocating carbon to roots. Proc Natl Acad Sci USA **103:** 12935–12940

Seifert GJ (2004) Nucleotide sugar interconversions and cell wall biosynthesis: how to bring the inside to the outside. Curr Opin Plant Biol **7:** 277–284

Shoresh M, Gal-On A, Leibman D, Chet I (2006) Characterization of a mitogen-activated protein kinase gene from cucumber required for trichoderma-conferred plant resistance. Plant Physiol **142:** 1169–1179

Sun JQ, Jiang HL, Li CY (2011) Systemin/jasmonate-mediated systemic defense signaling in tomato. Mol Plant **4:** 607–615

Takahashi F, Yoshida R, Ichimura K, Mizoguchi T, Seo S, Yonezawa M, Maruyama K, Yamaguchi-Shinozaki K, Shinozaki K (2007) The mitogen-activated protein kinase cascade MKK3-MPK6 is an important part of the jasmonate signal transduction pathway in *Arabidopsis*. Plant Cell **19:** 805–818

Tallamy DW (1985) Squash beetle feeding behavior: an adaptation against induced cucurbit defenses. Ecology **66:** 1574–1579

Thorpe MR, Ferrieri AP, Herth MM, Ferrieri RA (2007) 11C-imaging: methyl jasmonate moves in both phloem and xylem, promotes transport of jasmonate, and of photoassimilate even after proton transport is decoupled. Planta **226:** 541–551

Tolstikov VV, Fiehn O (2002) Analysis of highly polar compounds of plant origin: combination of hydrophilic interaction chromatography and electrospray ion trap mass spectrometry. Anal Biochem **301:** 298–307

Toroser D, Plaut Z, Huber SC (2000) Regulation of a plant SNF1-related protein kinase by glucose-6-phosphate. Plant Physiol **123:** 403–412

Turgeon R, Oparka K (2010) The secret phloem of pumpkins. Proc Natl Acad Sci USA **107:** 13201–13202

van Bel AJE, Gaupels F (2004) Pathogen-induced resistance and alarm signals in the phloem. Mol Plant Pathol **5:** 495–504

van de Ven WT, LeVesque CS, Perring TM, Walling LL (2000) Local and systemic changes in squash gene expression in response to silverleaf whitefly feeding. Plant Cell **12:** 1409–1423

van Dongen JT, Schurr U, Pfister M, Geigenberger P (2003) Phloem metabolism and function have to cope with low internal oxygen. Plant Physiol **131:** 1529–1543

Walz C, Giavalisco P, Schad M, Juenger M, Klose J, Kehr J (2004) Proteomics of curcurbit phloem exudate reveals a network of defence proteins. Phytochemistry **65:** 1795–1804

Wang P, Du Y, Li Y, Ren D, Song CP (2010) Hydrogen peroxide-mediated activation of MAP kinase 6 modulates nitric oxide biosynthesis and signal transduction in *Arabidopsis*. Plant Cell **22:** 2981–2998

Xoconostle-Cázares B, Xiang Y, Ruiz-Medrano R, Wang HL, Monzer J, Yoo BC, McFarland KC, Franceschi VR, Lucas WJ (1999) Plant paralog to viral movement protein that potentiates transport of mRNA into the phloem. Science **283:** 94–98

Yang ZP, Li HL, Guo D, Tian WM, Peng SQ (2012) Molecular characterization of a novel 14-3-3 protein gene (Hb14-3-3c) from *Hevea brasiliensis*. Mol Biol Rep **39:** 4491–4497

Zhang B, Tolstikov V, Turnbull C, Hicks LM, Fiehn O (2010) Divergent metabolome and proteome suggest functional independence of dual phloem transport systems in cucurbits. Proc Natl Acad Sci USA **107:** 13532–13537

Zhang CK, Yu XY, Ayre BG, Turgeon R (2012) The origin and composition of cucurbit "phloem" exudate. Plant Physiol **158:** 1873–1882

Zhang ZP, Baldwin IT (1997) Transport of [2-^{14}C]jasmonic acid from leaves to roots mimics wound-induced changes in endogenous jasmonic acid pools in *Nicotiana sylvestris*. Planta **203:** 436–441

Zimmermann MR, Hafke JB, van Bel AJ, Furch AC (2012) Interaction of xylem and phloem during exudation and wound occlusion in *Cucurbita maxima*. Plant Cell Environ (in press)

Zuk M, Weber R, Szopa J (2005) 14-3-3 protein down-regulates key enzyme activities of nitrate and carbohydrate metabolism in potato plants. J Agric Food Chem **53:** 3454–3460